Dina H, Manaf K, Riyadh A. Development and experimental validation of a low-cost sensor system for structural health monitoring applications. 2026;27(3):2026313. https://doi.org/10.29354/diag/236890.

DIAGNOSTYKA, 2026, Vol. 27, No. 3

e-ISSN 2449-5220
DOI: 10.29354/diag/236890

DEVELOPMENT AND EXPERIMENTAL VALIDATION OF A LOW-COST SENSOR SYSTEM FOR STRUCTURAL HEALTH MONITORING APPLICATIONS

Dina Haider ALI *, Manaf Kadum Hussein Al-TALEB, Riyadh Abedraba ABBAS

Department of Electrical Engineering, College of Engineering, University of Wasit, Kut 52001, Iraq
* Corresponding author: Dinahaider59@gmail.com

Abstract

Structural Health Monitoring (SHM) enhances the safety and reliability of civil infrastructure through continuous assessment of structural conditions. However conventional SHM systems are often limited by high installation costs, complex hardware, and challenging implementation. This study presents the development and experimental validation of an integrated, low-cost SHM platform for reinforced concrete structures using conventional electrical resistance strain gauges. The platform combines a signal-conditioning circuit, an STM32-based data acquisition unit and a real-time monitoring interface into a practical SHM system. Experimental validation was conducted on a reinforced concrete slab subjected to progressively increasing compressive loading. Strain measurements from the proposed system were compared with those obtained using commercial DataTaker DT85G system. Performance of the system was evaluated using 326 paired measurement points based on Normalized Root Mean Square Error (NRMSE) and the Nash Sutcliffe Efficiency (NSE). The proposed platform achieving an NSE value of 98.86% and an NRMSE value of 3.3% demonstrates excellent agreement with commercial reference. These results confirm the accuracy and reliability of the developed platform for strain measurement. The proposed system provides reliable real-time strain monitoring while significantly reducing implementation costs and maintaining a simple hardware architecture making it a practical and cost-effective solution for long-term SHM applications.

Keywords: structural health monitoring; low-cost system; strain gauge; DataTaker DT85G; concrete slab.

List of Symbols/Acronyms

SHM – Structural Health Monitoring;
NSE – Nash-Sutcliffe Efficiency;
NRMSE – Normalized Root Mean Square Error;
GF – Gauge Factor;
ADC – Analog-to-Digital Converter;
CMRR – Common-Mode Rejection Ratio;
GUI – Graphical User Interface;
IoT – Internet of Things;
MCU – Microcontroller Unit;
WSN – Wireless Sensor Network;
ε – strain;
μ ε – Microstrain (10^{-6});

1. INTRODUCTION

Civil infrastructure, such as buildings and bridges, is continuously exposed to aging, harsh environmental conditions, earthquakes, overloads, and other external factors that gradually reduce its structural performance throughout its service life (1). If these changes are not detected in a timely manner (2), they may progress to severe structural damage (3), resulting in unexpected failures, significant economic losses (4), and serious risks to public safety (5). Therefore, ensuring the safety, reliability (6), and serviceability of civil structures has become a fundamental requirement for sustainable infrastructure management (7).

In this context, SHM has emerged as an effective engineering approach for continuously assessing the structural condition of civil infrastructure by integrating sensing technologies, data acquisition (8), and data analysis, enabling early damage detection, structural condition assessment, and timely maintenance planning (9).

Despite these operational advantages, the widespread implementation of SHM systems remains limited due to the high cost of commercial sensing devices and data acquisition systems, the large number of required cables (10), complex installation procedures, and long-term maintenance requirements (11).

In addition, conventional inspection techniques still rely heavily on visual inspection and manual procedures, making structural assessment time-consuming, subjective, and unsuitable for continuous monitoring

Among these parameters, strain measurement is considered one of the most reliable techniques

Received 2026-04-18; Accepted 2026-09-14; Available online 2029-09-16

for early damage detection because it provides direct information on structural deformation and strain redistribution. Furthermore (14), crack monitoring is an important indicator of structural deterioration, as crack initiation and propagation are the earliest visible signs of structural damage. Consequently, strain measurement plays a crucial role in evaluating structural safety (15).

In recent years, the accuracy of structural inspection and damage detection has significantly improved owing to advances in sensing technologies and intelligent image processing techniques. Nevertheless (16), despite these technological developments, several practical challenges still hinder the widespread adoption of SHM systems. Many existing monitoring systems rely on complex hardware configurations (17), specialized sensing components, and expensive commercial equipment, making them unsuitable for large-scale civil engineering applications or projects with limited budgets (18).

Furthermore, one of the major challenges in developing practical and reliable SHM systems is achieving high measurement accuracy while maintaining a simple hardware architecture and low implementation cost. Therefore, there is a continuing demand for low-cost sensing platforms (19) that provide accurate (20), reliable measurements without increasing system complexity or implementation costs (21).

Recent studies have demonstrated the feasibility of developing low-cost SHM systems using different approaches. Nilnoree et al (22) proposed a low-cost wireless sensor network for synchronized structural monitoring, Abazeed et al. (23) developed an ultra-low-cost wireless system for strain and displacement monitoring, and Dagsever et al. (24) developed a compact wireless multi-sensor platform for SHM.

Although these studies successfully demonstrated the potential of low-cost SHM technologies, they mainly focused on wireless communication, sensor synchronization, or multi-sensor integration. However, only a limited number of studies have validated their measurement accuracy through comparison with commercial reference systems. Consequently, the reliability of these system platforms and their suitability for engineering applications remain uncertain, particularly for long-term strain monitoring in reinforced concrete structures. Therefore, there is still a need for a fully integrated, low-cost SHM platform that combines reliable strain measurement, real-time monitoring, a dedicated signal-conditioning circuit, and rigorous experimental validation against a commercial reference system.

To address this research gap, the novelty of the present work lies in the development and experimental validation of a fully integrated, low-cost SHM platform. Specifically, the proposed platform integrates conventional electrical strain gauges, a custom-designed signal-conditioning circuit, an STM32-based data acquisition unit, and a real-time monitoring interface into a single practical monitoring system.

The performance of the proposed platform was experimentally validated through direct comparison with a commercial data acquisition system (DataTaker DT85G). The comparison demonstrated that the proposed platform provides a simpler hardware architecture, easier maintenance, lower implementation cost, and greater practicality for long-term structural monitoring while maintaining reliable measurement accuracy.

Accordingly, this study proposes a new low-cost SHM system based on conventional electrical strain gauges and an STM32 microcontroller for continuous strain monitoring. The proposed system was experimentally validated by directly comparing its response with that of a commercial data acquisition system under progressively increasing compressive loading, while evaluating the structural response throughout the different loading stages. The proposed system enables continuous strain monitoring in a practical, economical, and reliable manner. Furthermore, it provides a solid foundation for future integration with intelligent damage diagnosis techniques and wireless communication technologies, thereby supporting the development of advanced smart SHM applications.

2. MATERIALS AND METHODS

A low-cost SHM system was verified through comparative evaluations of multiple pilot tests conducted using a standardized SHM system (25). The pilot tests were conducted to verify the operational stability, measurement reliability, and proper functioning of the proposed low-cost SHM system, as well as to confirm its performance effectiveness.

2.1. Structural Integrity Monitoring Systems

SHM systems are advanced technologies designed to monitor the condition of structures, such as buildings, and to identify damage at an early stage, which is crucial for their safety and sustainability. Low-cost systems are designed to provide a quick, easy solution using inexpensive sensors and technology for broad use.

2.1.1. Low-Cost Structural Integrity Monitoring System

The measurement system proposed in this paper is capable of accurately obtaining and processing specific strain signals. As shown in Figure 1, the system starts with strain gauges wired in a Wheatstone bridge circuit that converts small changes in resistance due to mechanical deformation into a differential voltage output. A stable, constant current source of 50 mA was used to excite the bridge to improve measurement conditions. The resulting signal is then passed through a DC offset calibration stage to remove unwanted offset components and establish the baseline voltage level. Then, to suppress high-frequency noise, a first-order low-pass filter with a cutoff frequency of 10 Hz is applied. To further amplify the signal, a precision instrumentation amplifier (INA128) was used because the bridge output voltage is very small

It provides a high-precision, adjustable gain in the range of 100-1000. A reference voltage of 1.65 V was employed to bias the amplifier output within the ADC input range. Subsequently, the conditioned analog signal is converted into a digital signal by the STM32F103C8Tμ6 microcontroller for data acquisition and transmission of measured data to a computer for monitoring, processing, and storage.

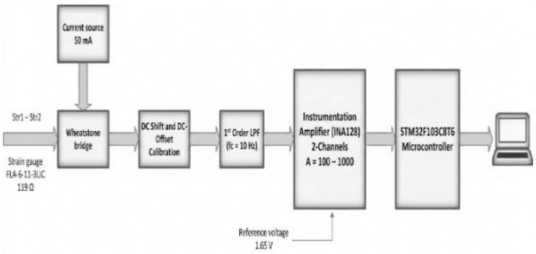

Fig. 1. System Block diagram

Figure 2 illustrates the analog signal-conditioning circuit used to interface low-level sensor signals with the STM32F103C8T6 microcontroller. The implementation of this proposed signal-conditioning architecture enables operational amplifiers, passive filtering elements, amplifier stages, and adjustable reference networks to achieve signal stability, noise immunity, and precision (26).

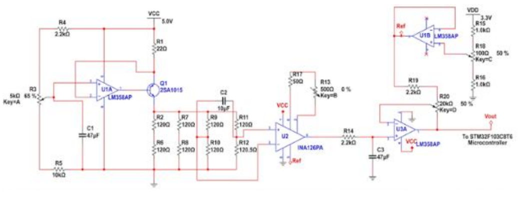

Fig. 2. Schematic diagram of the proposed strain gauge signal-conditioning circuit and data acquisition interface.

2.1.2. Signal Conditioning and Pre-Amplification

The proposed circuit employs an LM358 operational amplifier as the input signal-conditioning stage; when powered from a 5V supply, R3 and R5 form a variable-resistor network that lets the input bias and gain be tuned to suit different sensor levels. Capacitor C1 (47 μF) filters low-frequency noise and stabilizes the DC operating point. The next step uses a PNP transistor (2SA1015) to drive the pre-conditioning signal high enough to allow current to flow into the network, while keeping the voltage stable. Transistor Bias Network (R1–R4) maintains linear operation and thermal stability.

2.1.3. Differential Signaling and Noise Rejection

The introduced system is capable of rejecting common mode noise. This can be achieved by converting the processed signal into a differential signal using a balanced resistor network (R2–R12). This configuration also reduces signal distortion and electromagnetic interference (EMI), both of which are among the most common sources of measurement errors in industrial environments (26). The capacitance C2 (10 μF) helps smooth the DC voltage by shunting the remaining AC ripple. Thus, further suppressing it before it reaches the metering amplifier stage (27).

2.1.4. Amplifier Stage

The differential signal is amplified using the INA128 instrumentation amplifier. Standard resistor values were selected, and the amplifier gain was adjusted through resistor R13 according to the sensor sensitivity. The INA128 was chosen because of its high common mode rejection ratio (CMRR), excellent thermal stability, and low input offset voltage which enabling effective amplification of low-level signals. By applying a reference voltage (Ref) to the amplifier reference terminal, the output level is adjusted so that the differential input voltage matches the input range of the single ended analog to digital converter (ADC) of the microcontroller unit (MCU).

2.1.5. Output Calibration and Filtering

Finally, the amplified signal is processed by a second LM358 operational amplifier with a continuous-trim potential buffer and a low-pass filter. While R14, R19, and R20 form a network allowing output adjustment, C3 (47 μF) reduces high-frequency noise and transient disturbances. A variable-reference circuit composed of resistors R15, R16, and R18 provides a means to finely tune the output-voltage shift. This is to ensure that the maximum output signal does not exceed the ADC's stable operating range on the STM32 (0–3.3 V).

2.1.6. Microcontroller Interface

The processed analog output signal (V out) is directly sent to the ADC by the STM32F103C8T6 microcontroller, as shown in Figure 2. Such a circuit design can achieve lower output impedance, higher noise resistance, and stable voltage levels to ensure accurate digital sampling and reliable data acquisition.

The developed system, which was created for data acquisition of strain measurements as shown in Figure 3, consists of a sensor based on a

Wheatstone bridge and an analog signal-conditioning circuit that provides amplification and low-frequency filtering.

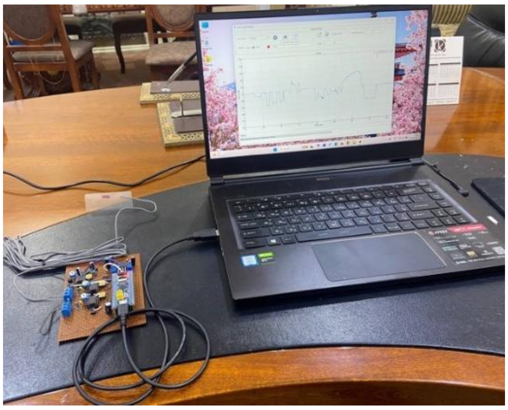

Fig. 3. SHM Platform Setup

Figure 4 shows the hardware implementation of the proposed SHM platform.

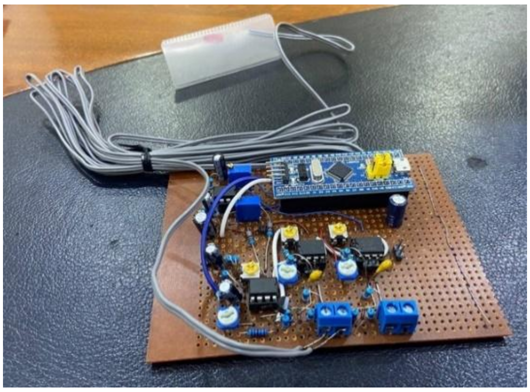

Fig. 4. SHM Platform Hardware Setup

An STM32 microcontroller is responsible for converting the signals into the digital domain, from which a graphical interface was designed for the PC to present immediate and reasoned results to the user, so it can save information, as shown in Figure 5. Suitable for use in experimental mechanical analysis, the system has high sensitivity, low noise, and adequate accuracy for force measurement.

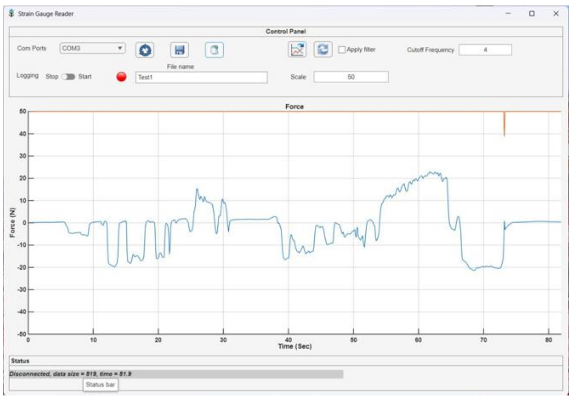

Fig. 5. System Graphical User Interface (GUI)

2.2. Theoretical Framework and Measurement Principles

Structural load monitoring systems rely on accurate strain measurements, which are the primary means of evaluating the safety and operational condition of engineering objects. Engineering strain (ε) is the ratio of the elongation (ΔL) to the initial length (L_0), as given by (28):

$$\varepsilon = \Delta L / L_0 \tag{1}$$

As the strains in SHM systems are considerably low, strain is expressed as microstrain (με), where 1με= 10^{-6} Strain. The microstrain unit provides a convenient and accurate representation of structural response under operating loads.

2.2.1. Measurement of Electrical Resistive Strain

Strain meters function by translating mechanical deformation into a change in the electrical resistance R, expressed as the relative change in resistance, ΔR/R. The gauge factor (GF) defines the sensitivity of a strain gauge.

$$GF = (\Delta R/R) / \varepsilon \tag{2}$$

Accordingly, the strain can be calculated directly from the change in resistance(29):

$$\varepsilon = (\Delta R/R) / GF \tag{3}$$

Commonly, a GF of about 2 enables foil-based strain gauges to indicate strain linearly or quasi-linearly as long as the deformation remains elastic. Recent advances in materials engineering have enabled the development of highly sensitive piezoelectric sensors, and shown that this technology can achieve far greater sensitivity than conventional gauges. Traditional gauges, however, remain more commonly used for SHM because they offer stability and high reproducibility. Strain gauges are normally connected in a Wheatstone bridge circuit to detect very small changes in resistance. The basic construction of a Wheatstone bridge includes four resistive arms excited by an excitation voltage Vex, and the imbalance behavior of a resistive arm under strain can be observed in the differential output voltage Vo. One of the bridge arms is an active strain gauge in a quarter-bridge arrangement, and the other three are constant resistors, as shown in Figure 6. In the case of small values of deformation, the output voltage can be expressed with the following formula:

$$Vo \approx Vex/4 \times GF \times \varepsilon \tag{4}$$

Rearranging the equation, we obtain:

$$\varepsilon = 4Vo / (Vex \times GF) \tag{5}$$

This equation establishes a direct connection between the measured electrical output and the applied mechanical strain; it is a standard equation in any practical strain-measurement system. Instrumentation amplifiers and signal-processing techniques improve measurement accuracy in practical applications.

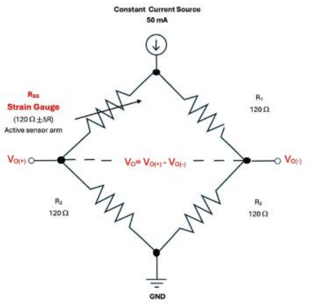

Fig. 6. Constant Current–Driven Quarter-Bridge Wheatstone Circuit for Strain Gauge Measurement

2.2.2. Structural Configuration and Reinforcement System

This study evaluated the flexural performance of a full-scale reinforced concrete slab specimen (2.0 m) subjected to laboratory loading. At the beginning of the specimen fabrication process, bottom and top reinforcement meshes were prepared, while polystyrene foam molds were placed in the central region to reduce the self-weight and create structural voids, as illustrated in Figure 7.

Fig. 7. Top view showing the reinforcement meshes and polystyrene blocks.

Subsequently, the concrete mixture was cast to form the rigid concrete slab. To establish an accurate framework for validating the final prototype of the SHM system, four electrical resistance strain gauges were installed at the center of the bottom reinforcement mesh and arranged as a sensor array, as shown in Figure 8.

Fig. 8. Top view indicating the locations of the strain gauges (SG1–SG4) attached to the bottom reinforcement mesh

The sensor array was divided into two equal groups. Two strain gauges were connected to the proposed low-cost SHM system whereas the other two were connected to the commercial high-cost data acquisition system as shown in Figure 9.

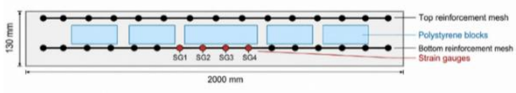

Fig. 9. Cross-sectional side view illustrating the internal arrangement of the concrete, reinforcement meshes, polystyrene blocks, and embedded strain gauges

This was used as the reference system for the experimental validation. This symmetrical arrangement facilitated the exposure of all four sensors to the same level of local mechanical strain variation during flexural loading thereby enabling a direct comparison of their performance in monitoring these variations.

2.2.3. Sample Preparation and Material Properties

In this study, a reinforced concrete slab was cast using self-compacting concrete (SCC) with a characteristic compressive strength of 40 MPa. The test specimen was prepared to represent the flexural response of a roof slab under simplified laboratory testing conditions. Its overall dimensions were 2.0 m in length, 630 mm in width, and 130 mm in depth, as illustrated in Figure 10. Concrete mixing and casting were carried out under carefully controlled laboratory conditions to obtain uniform mechanical properties and maintain the structural integrity of the specimen. The sample was cured for 28 days under standard curing conditions after casting to achieve its full strength prior to the test.

Fig. 10. Concrete Slab

2.2.4. Loading Protocol and Experimental Procedures

Using a mechanical loading device, progressively increasing quasi-static loads were applied to the concrete slab to simulate bending behavior, as shown in Figure 11. The loading stages were applied incrementally to monitor structural response at various load levels. Strain data were simultaneously recorded during the test by both the proposed system and a commercial reference device operating under similar loading conditions for comparison. The proposed system transmitted the measured data to a PC through the developed MATLAB graphical user interface (GUI), where the strain signals were displayed, recorded, and stored for subsequent analysis. During the experiment, 326 simultaneous comparison points were recorded. The commercial device sampled data at 10 Hz, so to achieve concordance with the proposed system's output (1 Hz), statistical averages were computed by reducing the sampling rate.

Fig. 11. Cracks developed in the concrete slab under applied load

2.2.5. Data Synchronization and Processing

To enable a direct comparison between the two measurement systems the recorded data were synchronized throughout all loading stages. In addition, signal alignment was carried out to eliminate any time discrepancies ensuring that each measurement point corresponded to the same loading condition.

Baseline correction and zero-offset calibration were applied before the test to reduce systematic errors and improve signal stability.

2.2.6. Performance Evaluation Metrics

The performance of the proposed low-cost SHM system was assessed by comparing the strain measurements with those obtained from the commercial DataTaker DT85G reference system. Two statistical performance metrics, namely the NRMSE and the NSE, were used to quantify the measurement error and evaluate the agreement between the proposed system and the commercial reference system. The statistical analysis was performed using MATLAB to evaluate the goodness of fit between the two datasets.

Their mathematical expressions are presented in Equations (6) and (7)

$$NRMSE = \frac{\sqrt{\frac{\sum_{i=1}^{L}(yoi-ypi)^2}{L}}}{yomax-yomin} \quad (6)$$

Where

y_{oi} is the reference strain measurement recorded by the commercial DataTakerDT85G system.

y_{pi} is the strain measurement obtained from the proposed low-cost SHM system.

$L$is the total number of paired measurements (326).

$y_{o\max}$and $y_{o\min}$are the maximum and minimum reference strain values, respectively.

Lower NRMSE values indicate better agreement between the proposed low-cost SHM system and the commercial reference system.

$$NSE = 1 - \frac{\sum_{i=1}^{L}(yoi-ypi)\hat{}2}{\sum_{i=1}^{L}(yoi-ymean)\hat{}2} \quad (7)$$

y_{mean}represents the mean value of the reference strain measurements.

The NSE ranges from negative infinity to 1. Values closer to 1 indicate excellent agreement between the strain measurements obtained from the proposed low-cost SHM system and those recorded by the commercial Data Taker DT85G reference system.

2.3.1. Reference data recorded

In this study, the Data Taker DT85G Geo Data Logger (Figure 12), a high-resolution commercial data collection system was employed as the reference tool for comparison with measurements from the IoT-based measurement system that was designed and developed. The DataTaker DT85G provides a wide range of features that meet the requirements of various scientific and engineering applications that requiring high measurement accuracy, multi-channel support, and reliable performance. It offers measurement accuracy of up to 18 bits and supports a variety of sensors including strain gauges, thermocouples, and linear variable differential transformers (LVDTs). Additionally, the device provides reliable signal processing which making it well suited for SHM and geotechnical measurement applications. Such data are typically acquired using commercial data loggers such as the DT85G which provides high stability and measurement accuracy for SHM applications. Furthermore, its Ethernet connectivity and support for widely used communication protocols, such as Modbus and FTP, enhance the reliability and integrity of data transmission. Remote access capabilities are also supported. According to industry measurement standards, the relatively high prices of such systems reflect their accuracy and durability.

Fig. 12. Data Taker DT85G Device

2.3.2. Economic Evaluation of the Proposed System Compared with the Commercial Data Acquisition Systems

Table 1 shows the proposed system implementation costs compared with commercial data acquisition systems while maintaining an adequate level of measurement accuracy. This reduction in cost represents a key advantage of the proposed system which demonstrating its potential as an economical alternative to conventional commercial measurement systems, particularly in cost-sensitive projects where the use of traditional systems is not economically feasible.

Table 1. Approximate Cost Comparison between the Proposed System and Commercial Data Acquisition Systems

System	Approximate Cost (USD)
Data Taker DT85G	≈ 5,100$
HBK Quantum X MX840B	≈ 6,000$
Proposed Low-Cost SHM System	**100$**

3. RESULTS AND DISCUSSIONS

The experimental results obtained from the strain gauges demonstrated a clear and consistent response under various loading conditions. The recorded measurements were analyzed and presented graphically to illustrate the axial strain values for the applied loads. Furthermore, a comparative evaluation was conducted between the statistical results obtained from the proposed system and the measurements recorded using the reference device to verify the accuracy of the proposed system. The results showed high agreement between the data sets, with only minor variations across all tested conditions. The measured data showed good consistency and remained within acceptable error limits. The comparison graph (Figure 13) illustrates the performance of the proposed IoT-based system relative to measurements from the Data Taker DT85G reference device. As shown in Figure 13, the experimental measurements showed good agreement with those obtained from the DT85G reference system.

The slight fluctuations observed during the loading process are attributed to sensor noise and environmental disturbances, but they remain within the acceptable engineering limits. Several recent studies propose such validation methods to ensure the accuracy of low-cost sensors compared to high-performance commercial solutions. Based on 326 paired measurements, the performance of the proposed SHM system was evaluated using two statistical performance metrics: NSE and the NRMSE. The proposed system achieved an NSE value of 98.86% and an NRMSE value of 3.3%, indicating excellent agreement with the commercial reference system and confirming the high accuracy and reliability of the proposed strain measurement system. Only the data recorded before the structural failure of the concrete slab were included in the statistical analysis, whereas the post-failure data were excluded because they do not represent the normal structural response. The obtained results confirm the reliability and effectiveness of the proposed system for real-time SHM applications.

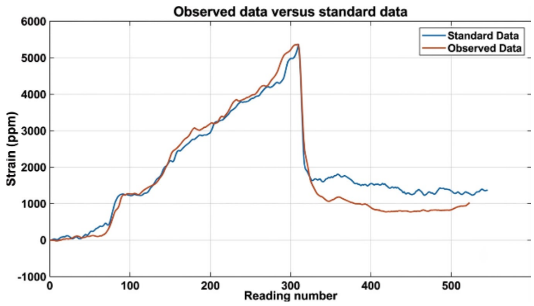

Fig. 13. Observed data versus standard data

3.1. Structural Response and Damage Development

Three critical stages of structural behavior were identified from recorded strain measurements, as shown in Figure 14. The system detected the onset of tensile strain development in the concrete section when the measured strain exceeded 400 με, indicating the initiation of structural deformation.

This strain level corresponds to the onset of the flexural response and the formation of micro-cracks, as evidenced by measurable elongation on the integrated strain gauge. The observation of tensile strain above this limit means that the slab has entered the cracking stage, confirming the flexural behavior of this structural element. As illustrated in the scatter plots, significant crack propagation occurred at approximately 2000 με, indicating the transition from microcracking to macro-scale structural failure.

This phase is characterized by a notable decline in rigidity and an elevation in stress localization within the tensile zones. Based on the behavior of reinforced concrete, a strain in this range indicates crack propagation and a loss of elastic response, corresponding to partial structural damage up to 0.65 times the ultimate load. Eventually, at a measured strain of approximately 3700 με, the entire structure failed, and the slab collapsed.

This strain corresponds to the element's maximum deformation capacity, indicating that damage exceeded the material's resistance limit. This represents a flexural failure in which the load-bearing capacity gradually decreases until it is ultimately lost.

As observed, the progression from initial cracking (400 microstrain) to final collapse (3700 microstrain) exhibits a typical pattern of damage propagation through the slab depth, confirming that the integrated strain monitoring system has captured an overall structural response spectrum ranging from the operational level to failure.

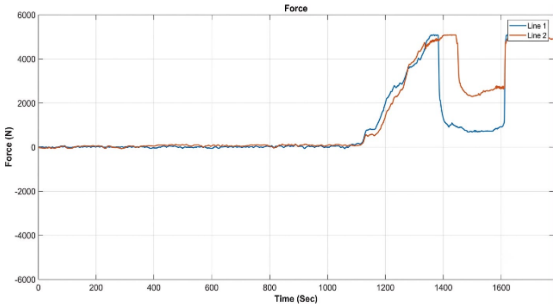

Fig. 14. Structural response of the concrete slab under applied loading

4. CONCLUSION

This study presented the development and experimental validation of an integrated low-cost SHM platform for concrete structures. The results demonstrate that the proposed system's accuracy is comparable to that of an expensive commercial data acquisition system, confirming that reliable real-time strain monitoring is possible without relying on costly, complex commercial SHM equipment.

One of the main limitations of this system, is currently designed to support a pair of strain sensors, making it suitable for small-scale structural monitoring applications. For use in larger, more complex structures, future hardware expansion will be required to support more strain sensors.

Moreover, intelligent techniques such as Fuzzy Logic can be incorporated to enhance the automated detection and classification of structural damage. In addition, the integration of GSM and GPS technologies can enable real-time remote monitoring based on the geographical location of the monitored structure. These developments are expected to improve the scalability of the proposed system while enhancing its practicality for real-world SHM applications.

Author Contributions: *Concept: M.K. R.A and D.H.; Methodology: D.H.; Software: R.A.; Validation: M.K., D.H., and R.A.; Formal Analysis: D.H.; Research: D.H.; Resources: RA and M.K.; Data Management: R.A.; Original Draft Writing: D.H.; Review and Editing: M.K.; Visualization: D.H.; Supervision: M.K.; Project Management; D.H. All authors have read and approved the published version of the manuscript.*

Funding: *This research did not receive any external funding.*

Institutional Review Committee Statement: *Not applicable.*

Informed Consent Statement: *Not applicable.*

Data Availability Statement: *The datasets generated and analyzed during this study are available from the responsible author upon request.*

Conflict of Interest: *The authors declare no conflicts of interest.*

Acknowledgments: *The authors extend their gratitude to the laboratories of the Civil Engineering Department and the Electrical Engineering Department, College of Engineering, University of Wasit, for their support of this study.*

REFERENCES

1. Zhang M, Liu Z, Shen C, Wu J, Zhao A. A review of radio frequency identification sensing systems for structural health monitoring. Materials (Basel). 2022;15(21):7851. https://doi.org/10.3390/ma15217851.
2. Cha YJ, Ali R, Lewis J, Büyüköztürk O. Deep learning-based structural health monitoring. Autom Constr. 2024;161:105328. https://doi.org/10.1016/j.autcon.2024.105328.
3. Wan S, Guan S, Tang Y. Advancing bridge structural health monitoring: Insights into knowledge-driven and data-driven approaches. J Data Sci Intell Syst. 2024;2(3):129–40. https://doi.org/10.47852/bonviewJDSIS3202964.
4. Tokognon CA, Gao B, Tian GY, Yan Y. Structural health monitoring framework based on Internet of Things: A survey. IEEE Internet Things J. 2017;4(3):619–35. https://doi.org/10.1109/JIOT.2017.2664072.
5. Plevris V, Papazafeiropoulos G. AI in structural health monitoring for infrastructure maintenance and safety. Infrastructures. 2024;9(12):225. https://doi.org/10.3390/infrastructures9120225.
6. Rahita AC, Zaki A, Nugroho G, Yadi S. Internet of Things (IoT) in Structural Health Monitoring: A Decade of Research Trends. Instrumentation, Mes Métrologies. 2024;23(2). https://doi.org/10.18280/i2m.230205.
7. Sun Z, Jayasinghe S, Sidiq A, Shahrivar F, Mahmoodian M, Setunge S. Approach towards the development of digital twin for structural health monitoring of civil infrastructure: A comprehensive review. Sensors. 2024;25(1):59. https://doi.org/10.3390/s25010059.
8. Mardanshahi A, Sreekumar A, Yang X, Barman SK, Chronopoulos D. Sensing techniques for structural health monitoring: A state-of-the-art review on performance criteria and new-generation technologies. Sensors. 2025;25(5):1424. https://doi.org/10.3390/s25051424.
9. Nayak R, Cleveland D, Joseph F. Characterization of sustainable bacterial cellulose fabricated with Vietnamese ingredients for potential textile applications: tensile and handle properties. Results Eng. 2025;25:104030. https://doi.org/10.1016/j.rineng.2025.104030.
10. Abdulkarem M, Samsudin K, Rokhani FZ, A Rasid MF. Wireless sensor network for structural health monitoring: A contemporary review of

technologies, challenges, and future direction. Struct Heal Monit. 2020;19(3):693–735. https://doi.org/10.1177/1475921719854528.

11. Elsisi A, Zamrawi A, Emad S. A Comprehensive Review of Structural Health Monitoring for Steel Bridges: Technologies, Data Analytics, and Future Directions. Appl Sci. 2025;15(22):12090. https://doi.org/10.3390/app152212090.
12. Avci O, Abdeljaber O, Kiranyaz S, Hussein M, Gabbouj M, Inman DJ. A review of vibration-based damage detection in civil structures: From traditional methods to Machine Learning and Deep Learning applications. Mech Syst Signal Process. 2021;147:107077. https://doi.org/10.1016/j.ymssp.2020.107077.
13. Meoni A, D Alessandro A, Mancinelli M, Ubertini F. A multichannel strain measurement technique for nanomodified smart cement-based sensors in reinforced concrete structures. Sensors. 2021;21(16):5633. https://doi.org/10.3390/s21165633.
14. Golding VP, Gharineiat Z, Munawar HS, Ullah F. Crack detection in concrete structures using deep learning. Sustainability. 2022;14(13):8117. https://doi.org/10.3390/su14138117.
15. Pereira L, Bourgeois I, Rodrigues H, Varum H, Antunes P. Fiber Bragg grating based displacement sensors with low visual impact for structural health monitoring applications–Monastery of Batalha case. Sensors Actuators A Phys. 2024;368:115117. https://doi.org/10.1016/j.sna.2024.115117.
16. Olivera J, González M, Fuente JV, Varga R, Zhukov A, Anaya JJ. An embedded stress sensor for concrete SHM based on amorphous ferromagnetic microwires. Sensors. 2014;14(11): 19963–78. https://doi.org/10.3390/s141119963.
17. Jia Z, Ma G, Su X, Li Y, Xing C, Ye S, et al. Development of a novel adaptive range strain sensor for structural crack monitoring. J Mar Sci Eng. 2022;10(11):1710. . https://doi.org/10.3390/jmse10111710.
18. Krishnan SSR, Karuppan MKN, Khadidos AO, Khadidos AO, Selvarajan S, Tandon S, et al. Comparative analysis of deep learning models for crack detection in buildings. Sci Rep. 2025;15(1):2125. https://doi.org/10.1038/s41598-025-85983-3.
19. Yuan Q, Shi Y, Li M. A review of computer vision-based crack detection methods in civil infrastructure: Progress and challenges. Remote Sens. 2024;16(16):2910. https://doi.org/10.3390/rs16162910.
20. Chen W, Hou J, Wang Y, Yu M. Visualization analysis of concrete crack detection in civil engineering infrastructure based on knowledge graph. Case Stud Constr Mater. 2024;21:e03711. https://doi.org/10.1016/j.cscm.2024.e03711.
21. Zhang X, Porro RP, Xu J, Zhu H, Li Z. A review of smartphone sensing for structural health monitoring. J Civ Struct Heal Monit. 2026;16(2): 17. https://doi.org/10.1007/s13349-025-01037-2.
22. Nilnoree S, Taparugssanagorn A, Kaemarungsi K, Mizutani T. Enhancing Wireless Sensor Network in Structural Health Monitoring through TCP/IP Socket Programming-Based Mimic Broadcasting: Experimental Validation. Appl Sci. 2024;14(8): 3494. https://doi.org/10.3390/app14083494.
23. Abazeed A, Abdelshakor M, Othman A, Tee KF, Lorenzana A. Development of an ultra-low-cost wireless data acquisition system for monitoring strain and deflection. J strain Anal Eng Des. 2025;60(3):196–207. https://doi.org/10.1177/03093247241293865.
24. Dagsever F, Sharif Khodaei Z, Aliabadi MHF. WSN-Based Multi-Sensor System for Structural Health Monitoring. Sensors. 2025;25(14):4407.
25. Shin KS, Nam Y, Suh YJ. Designing a Multivariate Belt Conveyor Idler Stall Detection and Identification System with Scalability Analysis. Sensors. 2024;24(24):7989. https://doi.org/10.1063/5.0270845.
26. Dhrubo AFH, Qayum MA. STM32-based IoT framework for real-time environmental monitoring and wireless node synchronization. arXiv Prepr arXiv250617295. 2025;
27. Yu Z, Zhang B. The art of noise modeling and mitigation on power line communication in distributed energy system. IEEE Trans Instrum Meas. 2025;
28. Kang X, Zhu B, Cai Y, Xiao Y, Liu N, Guo Z, et al. A concise review of state-of-the-art sensing technologies for bridge structural health monitoring. Sensors. 2025;25(17):5460.
29. Zike S, Mikkelsen LP. Correction of gauge factor for strain gauges used in polymer composite testing. Exp Mech. 2014;54(3):393–403.

Dina Haider Ali received her B.Sc. degree in Electrical Engineering from the College of Engineering, University of Wasit, Iraq, in 2021. She is currently an M.Sc. candidate in Electrical Engineering at the same institution. Her research interests include structural health monitoring, Internet of Things (IoT)-based sensor networks, electrical resistance strain measurement, embedded systems, data acquisition, real-time monitoring, and intelligent monitoring systems. eDinahaider59@gmail.com

Dr. Manaf Kadum Hussein Al-Taleb is an Assistant Professor in the Department of Electrical Engineering at the College of Engineering, University of Wasit, Iraq. He received his Ph.D. from the University of Glasgow, UK, for research on the development and clinical testing of home-based brain-computer interfaces for neurofeedback and rehabilitation. His research interests include brain-computer interfaces (BCI), neurofeedback, functional electrical stimulation, data acquisition and measurement systems, biomedical signal processing, artificial intelligence, and neurorehabilitation. His research also focuses on

the design and development of data acquisition systems for recording, processing, and analyzing biomedical signals, with applications in healthcare, rehabilitation, intelligent diagnostic systems, and Internet of Things (IoT) systems. Manaf@uowasit.edu.iq

Dr. Riyadh A. Abbas is a Senior Lecturer in the Department of Electrical Engineering at the College of Engineering, University of Wasit, Iraq. He received his B.Sc. degree in Electrical Engineering from Al-Mustansiriyah University, Iraq, in 1996, and his M.Sc. degree in Electronics and Communications from Al-Mustansiriyah University in 1999. He received his Ph.D. degree in Electronics and Communications from the University of Northampton, UK, in 2019. He has more than 20 years of experience in teaching and research in electronics and electrical engineering. His research interests include power electronics, FPGA-based systems, embedded systems, wireless communications, and Internet of Things (IoT) systems. Riyadhabbas@uowasit.edu.iq